RAD51 Foci as a Biomarker Predictive of Platinum Chemotherapy Response in Ovarian Cancer

Amanda J. Compadre[1], Lillian N. van Biljon[1], Mark C. Valentine[1], Alba Llop-Guevara[2], Emily Graham[1], Bisiayo Fashemi[1], Andrea Herencia-Ropero[2,3], Emilee N. Kotnik[1], Isaac Cooper[1], Shariska P. Harrington[4], Lindsay M. Kuroki[1], Carolyn K. McCourt[1], Andrea R. Hagemann[1], Premal H. Thaker[1], David G. Mutch[1], Matthew A. Powell[1], Lulu Sun[5], Nima Mosammaparast[5], Violeta Serra[2], Peinan Zhao[6], Elena Lomonosova[1], Dineo Khabele[1], and Mary M. Mullen[1]

ABSTRACT

Purpose: To determine the ability of RAD51 foci to predict platinum chemotherapy response in high-grade serous ovarian cancer (HGSOC) patient-derived samples.

Experimental Design: RAD51 and γH2AX nuclear foci were evaluated by immunofluorescence in HGSOC patient-derived cell lines ($n = 5$), organoids ($n = 11$), and formalin-fixed, paraffin-embedded tumor samples (discovery $n = 31$, validation $n = 148$). Samples were defined as RAD51-High if >10% of geminin-positive cells had ≥5 RAD51 foci. Associations between RAD51 scores, platinum chemotherapy response, and survival were evaluated.

Results: RAD51 scores correlated with *in vitro* response to platinum chemotherapy in established and primary ovarian cancer cell lines (Pearson $r = 0.96$, $P = 0.01$). Organoids from platinum-nonresponsive tumors had significantly higher RAD51 scores than those from platinum-responsive tumors ($P < 0.001$). In a discovery cohort, RAD51-Low tumors were more likely to have a pathologic complete response (RR, 5.28; $P < 0.001$) and to be platinum-sensitive (RR, ∞; $P = 0.05$). The RAD51 score was predictive of chemotherapy response score [AUC, 0.90; 95% confidence interval (CI), 0.78–1.0; $P < 0.001$). A novel automatic quantification system accurately reflected the manual assay (92%). In a validation cohort, RAD51-Low tumors were more likely to be platinum-sensitive (RR, ∞; $P < 0.001$) than RAD51-High tumors. Moreover, RAD51-Low status predicted platinum sensitivity with 100% positive predictive value and was associated with better progression-free (HR, 0.53; 95% CI, 0.33–0.85; $P < 0.001$) and overall survival (HR, 0.43; 95% CI, 0.25–0.75; $P = 0.003$) than RAD51-High status.

Conclusions: RAD51 foci are a robust marker of platinum chemotherapy response and survival in ovarian cancer. The utility of RAD51 foci as a predictive biomarker for HGSOC should be tested in clinical trials.

Introduction

Most patients with high-grade serous ovarian cancer (HGSOC) are diagnosed with advanced-stage disease for which the standard treatment includes platinum chemotherapy, and up to 80% of patients are candidates to receive maintenance therapy with PARP inhibitors (PARPis; refs. 1, 2). Carboplatin and PARPis cause double-stranded DNA (dsDNA) breaks. If a cell is incapable of completing homologous recombination (HR; e.g., in tumors with dysfunctional BRCA1, BRCA2), then it instead undergoes nonhomologous end-joining, leading to accumulated genotoxicity. Thus, HR-deficient tumors are more susceptible to DNA break-inducing agents than HR-proficient tumors.

Current clinical assays to predict HR capabilities of tumors include germline or somatic mutation testing of genes involved in HR, specifically *BRCA* and evaluation of a genomic scar that reflects the genomic instability resulting from HR deficiency (3). A genomic scar can be detected by measuring loss of heterozygosity (LOH) or calculating an HR deficiency index (HRDi) score (4, 5). Although such assays are commonly used to identify patients with HR defects, they reflect past events and do not necessarily reflect the current HR capacity of the tumor. Furthermore, they do not consider reversion mutations, epigenetic modifications, hypomorphic BRCA proteins, alternative splicing, or other resistance mechanisms that affect platinum and PARPi sensitivity. To minimize unnecessary toxicity and rationally triage patients to therapy, we need an assay that reflects current tumor response to DNA-damaging chemotherapeutic agents.

Here, we assessed the utility of an assay that reflects the current ability of tumors to perform HR. The DNA repair protein RAD51 is an optimal biomarker for such an assay for several reasons. First, upon a double-strand break (DSB) in DNA, the kinase ATM rapidly phosphorylates histone H2AX (γH2AX). This activates a signaling cascade that generates single-stranded DNA with 3′ overhangs. These overhangs are bound by replication protein A, which is ultimately replaced by RAD51 via mediator proteins, including BRCA1 and BRCA2. Finally, sister chromatid strand invasion and DNA synthesis lead to faithfully repaired DNA. Because many upstream events must occur for RAD51 to bind to DNA, and RAD51 is necessary to complete HR,

[1]Division of Gynecologic Oncology, Department of Obstetrics and Gynecology, Washington University, St Louis, Missouri. [2]Experimental Therapeutics Group, Vall d'Hebron Institute of Oncology, Barcelona, Spain. [3]Department of Biochemistry and Molecular Biology, Autonomous University of Barcelona, Barcelona, Spain. [4]Minnesota Oncology, St. Paul, Minnesota. [5]Department of Pathology and Immunology, Washington University, St. Louis, Missouri. [6]Department of Obstetrics and Gynecology, Center for Reproductive Health Sciences, Washington University, St Louis, Missouri.

A.J. Compadre and L.N. van Biljon contributed equally as co-authors of this article.

Corresponding Author: Mary M. Mullen, Washington University in St. Louis School of Medicine, St. Louis, MO 63122. Phone: 314-640-1324; Fax: 314-747-0264; E-mail: marymullen@wustl.edu

Clin Cancer Res 2023;29:2466–79

doi: 10.1158/1078-0432.CCR-22-3335

Translational Relevance

Current biomarkers to predict response to standard-of-care platinum chemotherapy in high-grade serous ovarian cancer (HGSOC) have limited accuracy. Here, we show that a reliable and reproducible RAD51 foci assay can predict platinum chemotherapy response in established and patient-derived ovarian cancer cell lines, patient-derived organoids, and pretreatment formalin-fixed, paraffin-embedded tumor biopsies. Furthermore, we present a novel automated system to quantify this assay to facilitate translation into clinical care. In a validation cohort of 148 patients, the automated assay demonstrates 100% specificity and 100% positive predictive value in predicting platinum sensitivity. In multivariate analysis, this RAD51 foci assay also predicts survival. This work provides the preclinical rationale for a large prospective clinical trial to validate RAD51 foci as a predictive biomarker in HGSOC.

RAD51 provides a comprehensive readout for many independent steps of HR. Second, upon binding, RAD51 forms a nucleoprotein filament that can be visualized microscopically as foci, and the inability to form RAD51 foci has been used as a functional marker of HR deficiency (6–8). Third, RAD51 foci assays predicted response to platinum chemotherapy and to PARPis in patient-derived breast and ovarian cancer xenografts (9–11). Similarly, quantification of RAD51 foci in breast cancer patient samples predicted response to platinum chemotherapy (12, 13). However, whether RAD51 foci can accurately predict response to platinum chemotherapy in readily available HGSOC formalin-fixed paraffin-embedded (FFPE) patient tumor samples is unknown. Furthermore, RAD51 foci in FFPE are currently quantified manually, limiting translation into clinical care. Here, we rigorously test this biomarker in patient-derived cell lines, organoids, and FFPE samples. Furthermore, we describe a novel automated quantification method and show its accuracy in both a discovery cohort and a validation cohort. We demonstrate that automated quantification of RAD51 foci is a robust and reliable method to accurately predict HGSOC patient response to platinum chemotherapy and survival in clinically available samples.

Materials and Methods

Patient population

Tissues for primary ovarian cancer cell and organoid generation were collected prospectively as part of our Gynecologic Oncology biorepository (IRB No. 201105400 and IRB No. 201706151) after obtaining patient consent.

Tissues for formalin fixation and paraffin embedding were collected prospectively (IRB No. 201407156) as part of a National Cancer Institute-funded project studying patients with advanced-staged HGSOC undergoing neoadjuvant chemotherapy. Patients were included if they had stage III–IV HGSOC and underwent neoadjuvant chemotherapy and interval cytoreductive surgery. Tissue specimens were collected before neoadjuvant chemotherapy. Chemotherapy response was assessed at the time of interval cytoreductive surgery and defined according to a validated histopathologic scoring system (14–19). A chemotherapy response score of 1 was considered little to no response and 3 was considered a pathologic complete response (pCR). Progression-free survival (PFS) and overall survival (OS) were calculated from the time of interval cytoreductive surgery.

FFPE ovarian cancer tissue microarrays were obtained from the University of Kansas and the Anatomic and Molecular Pathology Core Laboratories at Washington University. The microarrays contained normal, primary, and metastatic tumors from patients with HGSOC. Samples were obtained at primary or interval cytoreductive surgery after platinum chemotherapy. *BRCA* mutation status was reported, but status of the mutation (benign vs. pathogenic) was unknown. Platinum chemotherapy resistance was defined as recurrence within 6 months of completing platinum chemotherapy.

This study was conducted in accordance with guidelines set forth by the Belmont Report. All patients provided written informed consent.

DNA/RNA sequencing, BRCA status, LOH, HRDi, DNA repair genes

All tumors were examined by a pathologist to determine tumor cellularity and necrosis, and only samples of 60% tumor cellularity or higher with <20% necrosis were sequenced. DNA and RNA were extracted from tumors embedded in optimal cutting temperature compound tissues using Qiagen's DNeasy Blood and Tissue Kit (cat No. 69504) according to the manufacturer's protocol. Samples underwent whole-genome sequencing (WGS) to an average depth of 30X. Reads were aligned with bwa (version 0.7.8) and duplicates were removed with picard-tools (version 2.21.7). Base quality recalibration was performed per GATK best practices. Somatic variants were called using Mutect-2 with Gnomad variants as a germline resource and filtered using GATK (version 4.1.9.0). LOH, telomeric allelic imbalance, and large-scale transitions, were calculated with ascatNGS (version 2.1.1) as previously described (20), and these values are added to generate the HRDi score as a proxy for the commercially available Myriad myChoice assay (21). A high HRDi score was considered any value ≥42 and a high LOH score ≥16 as previously described (22–25). Germline and somatic DNA data regarding *BRCA* status were obtained from next-generation sequencing (NGS) gene panel tests obtained as standard-of-care.

RNA sequencing of primary tumor samples was performed using the Illumina TruSeq stranded Total RNA library kit following the recommended protocol, with paired-end Illumina sequencing of 151 bp read length, with an average of approximately 125 million paired reads per sample and an average of approximately 134 million reads mapped per sample. Transcript quantification was performed using kallisto (26). Downstream analysis was then performed in R.

Cell lines

ES2 (cultured in McCoys plus 10% FBS and 1% penicillin and streptomycin) and OVCAR8 cells (cultured in RPMI plus 10% FBS and 1% penicillin and streptomycin) were obtained from the National Cancer Institute. COV362 and TykNu cells (Sigma-Aldrich) were cultured in DMEM plus 10% FBS, 1% L-Glutamine, and 1% penicillin and streptomycin. PEO1 and PEO4 cells (Sigma-Aldrich) were cultured in RPMI plus 10% FBS. UWB1 and UWB1+B1 cell lines were generously provided by Lee Zhou (Massachusetts General Hospital Cancer Center, Harvard Medical School), and cultured in a 1:1 ratio of RPMI and MEGM BulletKit (Lonza) supplemented with 3% FBS and 1% penicillin and streptomycin. All cells were maintained at 37°C in a 5% CO_2 incubator. Cell lines were confirmed mycoplasma negative with the MycoAlert *Mycoplasma* Detection Kit (Lonza) before experiments. Cells were used for 2 to 3 months then discarded.

Development of primary cell lines

To develop patient-derived ovarian cancer cells, ovarian cancer patient ascites were collected from patients with advanced-stage HGSOC, mixed in a 1:1 ratio with RPMI supplemented with 20% FBS and 1% penicillin and streptomycin, and cultured in flasks. After 7 to 14 days, the attached and proliferating cells were passaged and used for experiments. Primary cells were used for 1 to 2 passages then discarded.

Cell line immunofluorescence

Cells (40,000 per well) were plated in an 8-well chamber slide. Cells were then treated with 10 Gy of ionizing radiation at 37°C. After treatment, the cells were washed with cold PBS, fixed with 2% paraformaldehyde for 10 minutes, permeabilized with 0.2% Triton X-100 in PBS for 20 minutes, and then washed and blocked (30 minutes) with staining buffer (PBS, 0.5% BSA, 0.15% glycine, and 0.1% Triton-X-100). Cells were incubated overnight at 4°C with primary antibodies (Supplementary Table S1) in staining buffer. Cells were then stained with secondary antibodies (Supplementary Table S1) and DAPI (Sigma) and imaged using a Leica TCS SPE inverted confocal microscope. Raw images were exported, and foci were counted with JCountPro (27, 28). At least 100 cells were analyzed for each treatment group in duplicate.

Western blot analysis

Cultured cells were lysed in 9 mol/L urea, 0.075 mol/L Tris, pH 7.6, and proteins were quantified by the Bradford assay. Protein lysates (60–100 μg) were subjected to reducing SDS-PAGE by standard methods and transferred to a nitrocellulose membrane. Each membrane was probed with primary antibody at 4°C for 1 to 3 nights, washed, and probed with corresponding horseradish peroxidase–conjugated secondary antibodies (Supplementary Table S1). Signal was detected with the Pierce ECL Western Blotting Substrate, and chemiluminescence was measured on a ChemiDoc (Bio-Rad Laboratories).

FFPE-*transfected HGSOC cells*

ES2 and COV362 cells were transfected with RAD51 Silencer Select siRNA (Thermo Fisher Scientific, AM16708 and 4392420), or Negative Control siRNA (Qiagen, 1022076) using Lipofectamine RNAiMAX transfection reagent (Thermo Fisher Scientific) according to the manufacturer's instructions. The ES2 and COV362 cell lines were then irradiated at 10 Gy and incubated for 4 hours at 37°C. In addition, nontransfected ES2 and COV362 cells were exposed to varying amounts of ionizing radiation (0 Gy, 5 Gy, and 10 Gy). The cells were lifted off the plate and fixed in 4% paraformaldehyde for 1 hour. The cell pellet was embedded in 2% agarose and put into a cassette in 10% formalin for an additional 24 hours. The cell pellets were washed with deionized water and dehydrated in sequential concentrations of ethanol (30%, 50%, and 70%). The samples were embedded in paraffin wax, cut into 4-μm sections, and mounted onto slides.

Drug treatment and cell viability assays

Cells were seeded in a 96-well plate (2,000 cells per well) and incubated overnight before treatment with sequential dilutions of carboplatin (Teva Pharmaceuticals; range, 50–1,000 μmol/L) for 6 (ovarian cancer cell lines) or 7 (patient-derived ovarian cancer cells) days. Cell viability was assessed with MTS reagent that contains a tetrazolium compound [3-(4,5-dimethylthiazol-2-yl)-5-(3-carboxymethoxyphenyl)-2-(4-sulfophenyl)-2H-tetrazolium, inner salt; MTS] and an electron-coupling reagent (phenazine methosulfate; PMS). The optical density (absorbance at 490 nm) was measured with an Infinite M200 Pro plate reader (Tecan, Inc.). IC_{50} values were determined in GraphPad Prism (GraphPad Software, Inc.).

Organoid generation

Tumor biopsies and/or malignant ascites were collected from patients with HGSOC. For solid tumors, samples were manually minced then chemically and mechanically digested with the gentleMACS Octo Dissociator with Heaters (Miltenyi Biotec; No. 130096427), 2 mg/mL Type II Collagenase (Life Technologies; No. 17101015), and DNase (NEB; No. M0303S). Both the homogenate and the ascites cell pellet were filtered (Laboratory Source; No. T50476) and treated with DNase and red blood cell lysis buffer (BioLegend; No. 420301). Single-cell suspensions of tumor or ascites were resuspended in 75% Cultrex (R&D Systems; No. 353300502) and 25% organoid base media [Advanced DMEM/F12 (Thermo Fisher Scientific; No. 12634028) supplemented with 1% penicillin–streptomycin (Millipore Sigma; No. P0781), 1x Glutamax (Life Technologies; No. 35050061), and 1% HEPES (Life Technologies; No. 15630080)]. The cell suspension was plated onto a 6-well plate, in approximately 35-μL droplets, and placed into a 37°C incubator to solidify. The organoids were cultured in the base media plus 50 ng/mL EGF (PeproTech; No. 10026), 10 ng/mL FGF-10 (PeproTech; No. 10026), 10 ng/mL FGF2 (PeproTech; No. 100–18B), 1× B27 (Life Technologies; No. 17504044), 10 mmol/L nicotinamide (Sigma-Aldrich; No. N0636), 1.25 mmol/L N-acetylcysteine (Sigma-Aldrich; No. A9165), 1 μmol/L prostaglandin E2 (R&D Systems; No. 2296), 10 μmol/L SB202190 (Sigma-Aldrich; No. S7076), 500 nmol/L A83–01 (Sigma-Aldrich; No. SML0788), and 10 μmol/L ROCK inhibitor (R&D Systems, No. Y27632; ref. 29).

Organoids were classified as platinum-responsive or platinum-nonresponsive according to the parent tumor's CRS score (1–2: platinum-nonresponsive; 3: platinum-responsive) or their platinum-free interval (<6 months: platinum-nonresponsive; ≥6 months: platinum-responsive). *In vitro* carboplatin sensitivity was used when clinical data were not available ($n = 1$).

Organoid platinum sensitivity assays

For organoid carboplatin sensitivity assay, 20,000 cells per 10 μL of 75% Cultrex were plated into the wells of a black walled 96-well plate. On day 2, media containing 1, 5, 10, 25, 50, and 75 μmol/L of carboplatin (Teva; No. 00703424601) were added to the organoids. On day 7, an equal volume of CellTiter-Glo 3D Cell Viability Assay (Promega; No. G9681) was added to each well, and the luminescence was read using a Tecan plate reader. The percentage of cell viability was calculated and graphed using Microsoft Excel and GraphPad Prism.

Organoid immunofluorescence

Organoids were plated in Cultrex and cultured in an 8-chamber dish for 3 to 5 days. The organoids were treated with 10 Gy of ionizing radiation at 37°C and fixed with 2% paraformaldehyde for 10 minutes. They were then washed with staining buffer, permeabilized (PBS with calcium and magnesium, 0.2% Triton X-100) for 20 minutes, washed with staining buffer, and then blocked with staining buffer for 30 minutes. Organoids were incubated overnight at 4°C with primary antibodies (Supplementary Table S1), washed with staining buffer, stained with secondary antibodies (Supplementary Table S1) and DAPI (Sigma), and mounted with Prolong Gold Antifade Mountant (Sigma). Organoids were imaged on a Leica TCS SPE inverted confocal microscope. Raw images were exported, and foci were counted with JCountPro (27, 28). At least 100 cells were analyzed for each treatment group in duplicate.

FFPE immunofluorescence

Hematoxylin and eosin–stained slides of FFPE samples were screened for diagnosis, cellularity, and necrosis by a board-certified pathologist. Staining methods were adapted from Llop-Guevara and colleagues (13). FFPE blocks were cut into 4-μm sections and deparaffinized in organic solvents. Slides were dehydrated, submerged in DAKO Antigen Retrieval Buffer (pH 9.0), and incubated at 110°C in a steam rice cooker for 30 minutes. The slides were then cooled on ice for 30 minutes, followed by 5 minutes in distilled water. Samples were permeabilized with DAKO Wash Buffer for 5 minutes, then blocked with blocking buffer (DAKO Wash buffer; 1% BSA) for 5 minutes. The primary antibodies (Supplementary Table S1) were diluted in DAKO Antibody Dilutant and incubated for 1 hour. Then, samples were washed, blocked for 5 minutes, and incubated for 30 minutes in blocking buffer with secondary antibodies (Supplementary Table S1). DAPI (Sigma) was added, and the slides were dehydrated with increasing concentrations of ethanol. Samples were then mounted with prolong gold anti-fade reagent and stored at –20°C. Stained samples were imaged on a Leica Thunder Imager Microscope.

The amount of DNA damage was quantified by scoring the percentage of geminin-positive cells with 2 or more γH2AX foci. Only samples with a γH2AX score of >25% were evaluated for RAD51 to avoid false negatives as a result of inadequate dsDNA breaks to mount an HR response. RAD51 foci were quantified by scoring the percentage of geminin-positive cells with 5 or more RAD51 foci of approximately 3-μm diameter. At least 100 geminin-positive cells per sample were assessed. All samples were scored by 2 independent, masked reviewers. Tumors were defined as RAD51-Low if the RAD51 score was <10% and RAD51-High if the RAD51 score was >10%.

Automated foci analysis

Microscopy images from the RAD51 foci assay were imported into R environment. After denoising, smoothing, and thresholding, a 2-dimensional convolution was applied to segment all the foci in the image. Then, the cells were segmented by using a denoising and adaptive thresholding method, the foci-positive cells were counted, and the ratio to all cells was calculated. With multiple images from each patient, a median ratio was computed to estimate the RAD51 score. Using the linear coefficient of linear regression modeling, an automated cutoff value of 6% was determined to identify RAD51-High tumors.

Statistical analysis

Descriptive statistics were used to characterize baseline differences between patients. Missing data were excluded from the analysis. Categorical factors were compared between groups by using the χ^2 or Fisher exact test, as appropriate. Independent Student *t* and Mann–Whitney *U* tests were used to compare normally and nonnormally distributed continuous variables, respectively. One-way ANOVA was used as appropriate. Pearson rank correlation coefficient was used for correlation analyses. Sensitivity analysis was performed. Poisson regression was used to report relative risks (RRs). Areas under the receiver-operating characteristic curves were used to compare the predictive performance of RAD51 scores and genomic scars. PFS and OS were calculated as the time from surgery to physical or radiographic evidence of disease recurrence, date of death, or date of last contact if no recurrence occurred. Patients alive or without recurrence were censored at the date of last contact. Platinum resistance was defined as progression-free interval <6 months (30). The Kaplan–Meier method was used to estimate survival times, and distributions were compared using the log-rank test. Univariate and multivariate Cox proportional hazards regression analysis were used as indicated. Two-tailed 95% CIs and *P* values were calculated, and $P < 0.05$ was considered significant. GraphPad Prism 9 software and SPSS version 27 were used for statistical analysis and IC_{50} value calculations.

Sample size

On the basis of previously published research, we anticipated that at least 30% of tumors would be scored as RAD51-Low (11, 31, 32). Furthermore, from our institution's previous clinical trial evaluating neoadjuvant chemotherapy in ovarian cancer, we projected that 35% to 40% of patients would have a pCR. Therefore, the necessary sample size to detect a significant RR of having a pCR for the RAD51-Low patients was calculated (12, 32). If the expected RR of RAD51-Low was higher than 3.5, then 26 participants would provide the study with 80% power, at a 2-sided significance level of 0.05, including 11 (30%) patients with a RAD51-Low score and 24 (70%) patients with a RAD51-High score (33). A validation cohort of 148 patients was used to confirm the automated quantification methods developed in the discovery cohort.

Data availability

The data generated or used in this study will be made available upon request. Please contact the corresponding author for requests.

Results

RAD51 foci are associated with *in vitro* platinum chemotherapy response in ovarian cancer cell lines and patient-derived ovarian cancer cells

Upon binding to sites of DNA DSBs, RAD51 forms a nucleoprotein filament that can be visualized microscopically as foci, and the ability to form RAD51 foci has been suggested as a functional read-out for HR proficiency (6, 7). To determine whether RAD51 foci would predict platinum response independent of genomic HR status, we treated 8 established HGSOC cell lines—2 *BRCA1*/2 wild-type (WT), 2 *BRCA1* mutated, 1 *BRCA2* mutated, 1 *BRCA1* methylated, 1 *BRCA1* WT restored, and 1 with a *BRCA2* reversion mutation—with 10 Gy of radiation to cause DNA damage. We then used immunofluorescence to assess for the G2/S phase cell-cycle marker geminin, γH2AX foci (34), and RAD51 foci. We only analyzed samples in which >25% of geminin-positive cells had ≥5 γH2AX foci, indicating sufficient dsDNA breaks to mount an HR response. Therefore, only irradiated cells were analyzed. We assigned each cell line a RAD51 score—defined as the percentage of geminin-positive cells with ≥5 RAD51 foci—and found that RAD51 score correlated significantly with carboplatin IC_{50} value (Pearson $r = 0.92$, $P = 0.001$; **Fig. 1A** and **B**). In contrast, the γH2AX score did not correlate with carboplatin IC_{50} value ($P > 0.05$; Supplementary Fig. S2A). We performed the same evaluation in 5 patient-derived ovarian cancer cell cultures—3 platinum-resistant (progression-free interval <6 months) and 2 platinum-sensitive (progression-free interval ≥6 months; Supplementary Table S2; Supplementary Fig. S1). One patient had a *BRCA1* mutation. RAD51 foci, but not γH2AX foci, significantly correlated with carboplatin sensitivity *in vitro* (Pearson $r = 0.96$, $P = 0.01$; **Fig. 1C** and **D**; Supplementary Fig. S2B). Cells obtained from patients with platinum-resistant disease had higher RAD51 scores than those from patients with platinum-sensitive disease (87.4% vs. 69.9%). These data indicate that RAD51 foci might be a reliable marker of chemotherapy response in HGSOC.

Unlike RAD51 foci, we suspected that RAD51 total expression would not be associated with platinum chemotherapy response. We used the cancer cell line encyclopedia (35) to determine RAD51

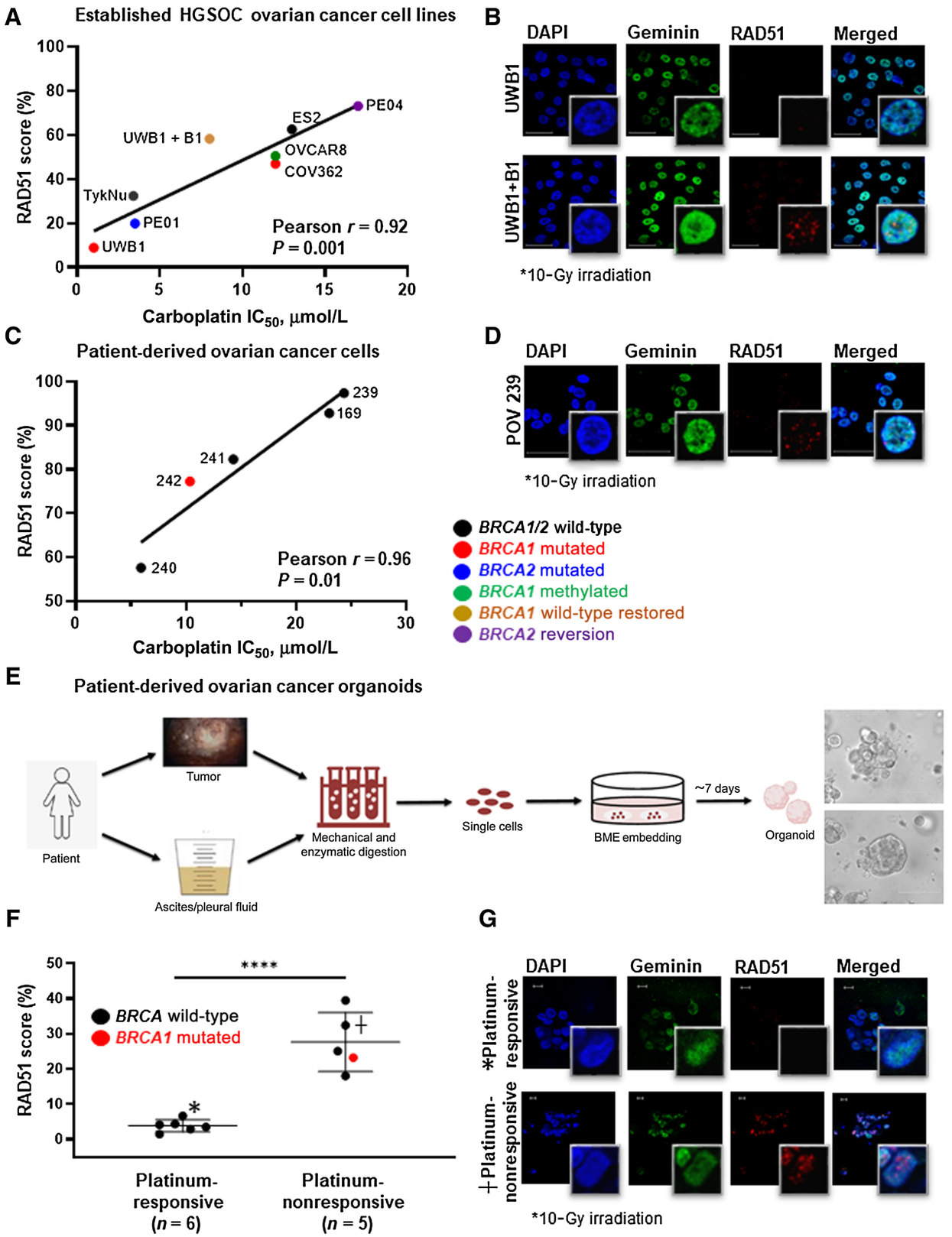

protein and mRNA abundance in 25 ovarian cancer cell lines and used the genomics of drug sensitivity database (www.cancerRxgene.org; ref. 36) to obtain cisplatin IC_{50} values for the same cell lines. RAD51 expression (quantified by reverse phase protein array, RT-PCR, or proteomics) did not correlate with cisplatin response or survival (Supplementary Fig. S3A and S3B). Moreover, using the Cancer Genome Atlas database, we found no difference in RAD51 expression between *BRCA* WT and mutated cells (Supplementary Fig. S3C). Thus, RAD51 abundance does not accurately predict platinum chemotherapy sensitivity in ovarian cancer.

RAD51 foci in patient-derived ovarian cancer organoids are predictive of clinical platinum chemotherapy response

We next examined whether RAD51 foci in patient-derived ovarian cancer organoids would predict patients' clinical responses to carboplatin (Supplementary Fig. S1). Tumor organoids are 3-dimensional models that recapitulate tumor cell clonal heterogeneity, the tumor microenvironment, and cell–cell and cell–matrix interactions. Thus, they are more clinically relevant than cell lines for evaluating drug sensitivity, functional biomarkers, and processes such as DNA damage response (29). We generated 11 patient-derived ovarian cancer organoids (**Fig. 1E**) from patients with stage IIIC or IV HGSOC and no prior therapy (Supplementary Table S3). One parent tumor had a pathogenic *BRCA* mutation. Organoids were classified as platinum-responsive ($n = 6$, 55%) or platinum-nonresponsive ($n = 5$, 45%) according to the corresponding patient's chemotherapy response score (3 = platinum-responsive, 1–2 = platinum-nonresponsive), progression-free interval (≥6 months = platinum-responsive, <6 months = platinum-nonresponsive), or *in vitro* sensitivity when clinical data were not available ($n = 1$). We irradiated the organoids and only analyzed those with a γH2AX score of >25% (percentage of geminin-positive cells with 5 or more γH2AX foci). Organoids were defined as RAD51-Low if ≤10% of geminin-positive cells had ≥5 RAD51 foci ($n = 6$, 54.5%) and RAD51-High if >10% of geminin-positive cells had ≥5 RAD51 foci ($n = 5$, 45.5%). All organoids from platinum-nonresponsive tumors were RAD51-High ($n = 5$, 100%), all organoids from platinum-responsive tumors were RAD51-Low ($n = 6$, 100%; **Fig. 1F** and **G**), and RAD51 scores were significantly higher in organoids from platinum-nonresponsive tumors than in organoids from platinum-responsive tumors (27.7% vs. 3.8%, $P < 0.001$; **Fig. 1F**). Organoids from platinum-responsive tumors had similar rates of γH2AX foci as organoids from platinum-nonresponsive tumors (Supplementary Fig. S2C and S2D). These data suggest that RAD51 foci correlate with clinical platinum chemotherapy response in patient-derived organoids.

The RAD51 foci assay is feasible and reliable in FFPE samples

Given the cost and time involved in generating primary ovarian cells and organoids, we next assessed the possibility of measuring RAD51 foci in FFPE tumor samples. **Fig. 2A** shows our workflow and scoring criteria, which were adapted from Llop-Guevera and colleagues (13). First, all FFPE samples must have a γH2AX score of >25%, indicating sufficient dsDNA breaks to mount RAD51 binding. Cells were then screened for geminin and RAD51 (RAD51 score). Per previously validated cutoff values established in patient-derived xenografts and patient breast cancer samples (9, 13), tumors were defined as RAD51-High if >10% of geminin-positive cells had ≥5 RAD51 foci and RAD51-Low if ≤10% of geminin-positive cells had ≥5 RAD51 foci (**Fig. 2A**). To assess the specificity of this assay, we knocked down RAD51 with two separate siRNAs in 2 HGSOC cell lines, 1 *BRCA* WT (ES2), and 1 *BRCA1* mutant (COV362; 37), embedded them in agarose, cut FFPE sections, and tested our methods and RAD51 antibody. We observed significantly fewer RAD51 foci in cells in which RAD51 was knocked down, both with and without irradiation (**Fig. 2B** and **C**). To assess the sensitivity of our assay, we irradiated RAD51-High HGSOC cell lines, embedded them in agarose, and tested our methods. With increasing doses of irradiation, the percentage of cells with RAD51 foci increased, demonstrating a broad dynamic range (**Fig. 2D**).

Having confirmed the sensitivity and specificity of our assay, we evaluated RAD51 foci in 31 HGSOC tumor biopsies obtained from primary tumor sites before the patients received neoadjuvant carboplatin and paclitaxel (**Fig. 2E**). All patients had advanced-stage disease (stage IIIC or IV) and at least mixed high-grade serous histology (**Table 1**). All patients had contributive testing results. We found discrete quantifiable foci that classified tumors as RAD51-High and RAD51-Low that allowed for formal analysis. In addition, using a subset of patients ($n = 17$), we compared 2 tumor samples obtained from different locations at the time same (**Fig. 2F**). There was high correlation between the 2 samples ($n = 17$, Pearson $r = 0.83$, $P < 0.001$, Cohen's Kappa coefficient 0.81, $P < 0.003$), indicating the results of this assay may not entirely depend on the biopsy location.

RAD51 foci in FFPE patient samples predict platinum chemotherapy response and survival

To investigate the accuracy of the RAD51 foci assay in predicting platinum chemotherapy response in patient-derived FFPE tumor samples, we evaluated the association between RAD51 scores and platinum chemotherapy response in pretreatment HGSOC tumor biopsies (**Fig. 3A**). Somatic and germline mutations in *BRCA1* and *BRCA2* were evaluated by standard-of-care NGS-based gene panel tests. Chemotherapy response was assessed at the time of interval cytoreductive surgery and defined according to a validated histopathologic scoring system (14–19). Thirteen out of 31 patients (41.9%) had a pCR (**Fig. 3A**). All FFPE patient tumors had a γH2AX score of >25%, indicating sufficient dsDNA breaks to cause RAD51 foci formation. Twelve (38.7%) tumors were RAD51-Low and 19 (61.3%) were

Figure 1.

RAD51 score correlates with platinum chemotherapy response in established and patient-derived ovarian cancer cell lines and patient-derived organoids. **A,** Correlation between RAD51 score (percentage of geminin-positive cells with ≥5 RAD51 foci) and carboplatin sensitivity (IC_{50}) determined by MTS assay in HGSOC cell lines. **B,** Representative images of geminin, RAD51, and colocalization of geminin/RAD51 at ×10 with ×63 insets in two established ovarian cancer cell lines. All foci were counted in 2 technical replicates with $n > 100$ geminin-positive cells per experiment; scale bars, 50 μm. **C,** Correlation between RAD51 score and carboplatin sensitivity (IC_{50}) determined by MTS assay in patient-derived HGSOC cell lines. **D,** Representative images of geminin, RAD51, and colocalization of geminin/RAD51 at ×10 with ×63 insets in 1 POV cell line. All foci were counted in 2 technical replicates with $n > 100$ geminin-positive cells per experiment; scale bars, 50 μm. **E,** Organoid generation from ovarian cancer tumor or ascites and representative brightfield microscopic image of ovarian cancer organoids after 7 days of growth; scale bars, 100 μm. **F,** RAD51 scores in platinum-responsive and platinum-nonresponsive patient-derived ovarian cancer organoids before and after irradiation. Error bars indicate ± SD. *, $P < 0.05$ and ****, $P < 0.0001$ by Student two-tailed *t* test. All foci were counted in 2 technical replicates with $n > 100$ geminin-positive cells per experiment. **G,** Representative images of geminin, RAD51, and colocalization of geminin/RAD51 at ×10 with ×63 insets; scale bars, 10 μm.

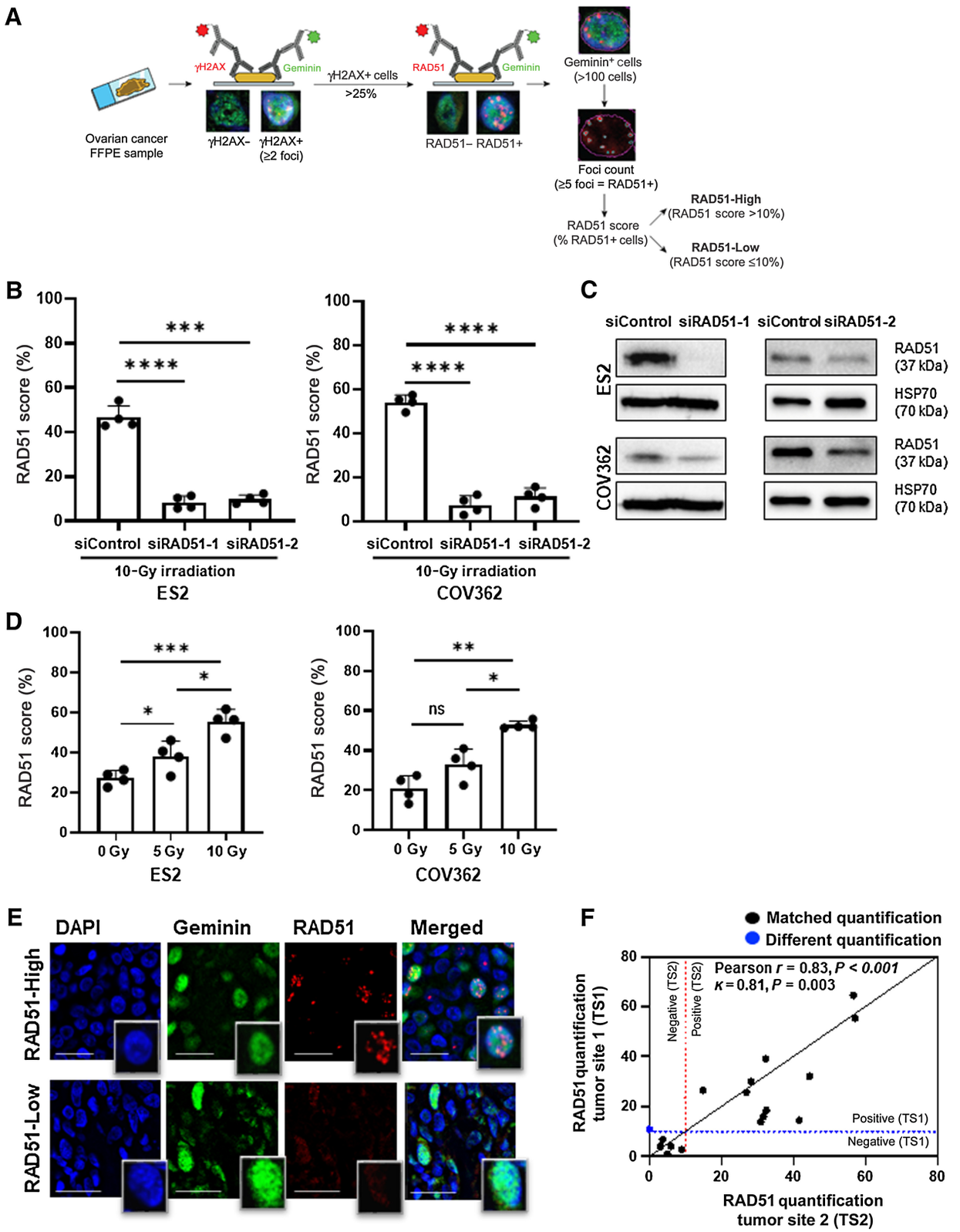

Table 1. Patient characteristics.

	Discovery Cohort ($n = 31$)	Validation Cohort[a] ($n = 149$)
Age, y	67.1 ± 10.1	67.4 ± 10.9
Race		—
Black	6 (19.4)	
White	25 (80.6)	
Other	0 (0)	
Primary site		
Ovary	24 (77.4)	147 (98.6)
Peritoneum	3 (9.7)	1 (0.7)
Fallopian tube	4 (12.9)	1 (0.7)
FIGO stage		
I	0	3 (2.0)
II	0	5 (3.4)
III	25 (80.6)	118 (79.2)
IV	6 (19.4)	23 (15.4)
BRCA mutation[b]		
None	21 (67.7)	57 (38.3)
BRCA1	6 (19.4)	36 (24.1)
BRCA2	1 (3.2)	18 (12.1)
No testing/missing	3 (9.7)	38 (25.5)
Chemotherapy Response Score (CRS)		
1–2	18 (58.1)	—
3 (pCR)	13 (41.9)	
Neoadjuvant chemotherapy		
Yes	31 (100)	23 (15.4)
No	0	126 (84.6)
Platinum sensitivity		
Sensitive (PFI ≥ 6 mo)	25 (80.6)	113 (75.9)
Resistant (PFI < 6 mo)	6 (19.4)	30 (20.1)
Missing	0	6 (4.0)
Residual disease at cytoreduction		
Absent	22 (71.0)	105 (70.4)
Present	7 (22.6)	22 (14.8)
Missing	2 (6.4)	22 (14.8)
PARP inhibitor Use		
Yes	7 (22.6)	27 (18.1)
No	24 (77.4)	118 (79.2)
Missing	—	4 (2.7)
Median follow-up (mo)	41.9 ± 22.7 (1.1 – 88.7)	51.2 ± 47.2 (1.0 – 276.0)

Note: Data are *n* (%) unless stated otherwise; ±, denotes standard deviation.
Abbreviation: PFI, progression-free interval.
[a]One patient with <25% γH2AX and so excluded from analysis.
[b]*BRCA* mutation status determined by germline testing or whole-genome sequencing. Limited information regarding pathogenicity of mutations.

RAD51-High (Supplementary Table S4). Pretreatment RAD51-Low tumors were more likely to have a pCR than RAD51-High tumors (RR, 5.28; 95% CI, 1.8–15.37; $P < 0.001$; **Fig. 3B**). In addition, RAD51-Low tumors were more likely to be platinum-sensitive than RAD51-High tumors (100% vs. 68%; $P = 0.03$; RR ∞, $P < 0.001$; **Fig. 3C**). The assay predicted platinum sensitivity with 100% specificity, 100% positive predictive value, and 48% sensitivity. Overall, RAD51 score was associated with survival (**Fig. 3D**) and predicted chemotherapy response (AUC, 0.90; 95% CI, 0.78–1.0; $P < 0.001$; **Fig. 3E**). Compared with patients with RAD51-High tumors, patients with RAD51-Low tumors had significantly longer PFS (17.5 months vs. 7.7; HR, 0.44; 95% CI, 0.20–0.98,-30.2; $P = 0.04$; **Fig. 3D**) and shorter OS (47.8 months vs. 36.2; HR, 0.49; 95% CI, 0.20–1.14; $P = 0.09$), though the latter was not significant (**Fig. 3D**).

A subset of patients ($n = 16$) underwent WGS (Supplementary Fig. S1). These sequencing data were used to infer LOH and an HRDi score, which combines LOH, telomeric allelic imbalance, and large-scale transitions (22). Nine (56.3%) tumors had a high HRDi score (≥42), and 7 (43.8%) had a low HRDi score (<42). Pretreatment genomic HRDi scores did not correlate with RAD51 scores ($r = 0.06$, $P = 0.83$).

Nine tumors with *BRCA* mutations were included—4 somatic *BRCA1* mutations, 2 germline *BRCA1* mutations, 1 somatic *BRCA2* mutation, and 1 germline *BRCA2* mutation. Five (55.5%) were RAD51-Low and 4 (44.4%) were RAD51-High. *BRCA*mutated, RAD51-Low tumors were more likely to have a pCR response than *BRCA* mutated, RAD51-High tumors (RR, 5.0; 95% CI, 0.87–28.86; $P = 0.04$). *BRCA*-mutated RAD51-Low tumors had significantly longer PFS (20.4 months vs. 7.8; $P = 0.02$) and OS (70.6 months vs. 36.7; $P = 0.03$) than patients with RAD51-High tumors (Supplementary Fig. S4A and S4B). In addition, limited RNA sequencing data ($n = 4$) suggested increased BRCA1 mRNA (22.3 vs. 6.1 transcripts per million) in a *BRCA1*-mutated, RAD51-High tumor compared with RAD51-Low tumors (Supplementary Fig. S4C). Immunofluorescence performed for BRCA1 on this same RAD51-High tumor demonstrated increased BRCA1 foci. In conclusion, our findings suggest that RAD51 score is a biomarker predictive of chemotherapy response in BRCA WT and *BRCA*-mutated FFPE HGSOC tumor samples.

To make the quantification of RAD51 foci in FFPE samples more objective, we used machine learning techniques such as denoising, filtering, and thresholding to develop an automated image processing method to segment and quantify the RAD51 staining images. We evaluated the discovery cohort both manually and by our automated quantification system. We found strong correlation between the 2 methods ($r = 0.72$, $P < 0.001$; Cohen's Kappa coefficient 0.86, $P < 0.001$; **Fig. 3F**; ref. 38). Automated quantification had accuracy of 93%, sensitivity of 100%, and specificity of 89%.

To validate automated RAD51 foci quantification as a biomarker, we performed immunofluorescence on two tissue microarrays ($n = 149$) containing high-grade serous ovarian, fallopian tube, or primary peritoneal tumors from patients receiving platinum chemotherapy (**Table 1**). The tissue microarrays contained primary, metastatic, and benign samples obtained at either primary or interval cytoreductive surgery (Supplementary Fig. S1). As an

Figure 2.
Validation of RAD51 immunofluorescence assay in formalin-fixed paraffin-embedded (FFPE) samples. **A,** RAD51 immunofluorescence assay in high-grade serous ovarian cancer (HGSOC) FFPE tumor samples. **B,** RAD51 scores in 2 HR-proficient HGSOC cell lines after transfection with 2 separate short-interfering RNA (siRNA) targeting RAD51 (siRAD51) or a noncoding region (siControl) and exposed to γ-irradiation. Cells were treated, fixed, embedded, and cut into 4-μm sections for evaluation. All foci were counted in 4 technical replicates with $n > 100$ geminin-positive cells per experiment. **C,** Western blot of the HGSOC cell lines after transfection with two siRNA (siRAD51–1: 121401; siRAD51–2: s531930) targeting RAD51. **D,** Dynamic range of RAD51 scores in 2 FFPE HR-proficient HGSOC cell lines after treatment with 0, 5, and 10 Gy of γ-irradiation. *, $P < 0.05$; **, $P < 0.01$; ***, $P < 0.001$; ****, $P < 0.0001$ by the Student two-tailed *t* test. **E,** Representative images of geminin, RAD51, and colocalization of geminin/RAD51 at ×10 with ×63 insets in a patient-derived FFPE HGSOC sample. All foci were counted in $n > 100$ geminin-positive cells per experiment; scale bars, 50 μm. **F,** Correlation in HGSOC FFPE tumor samples between RAD51 scores obtained from 2 separate samples from the same patient.

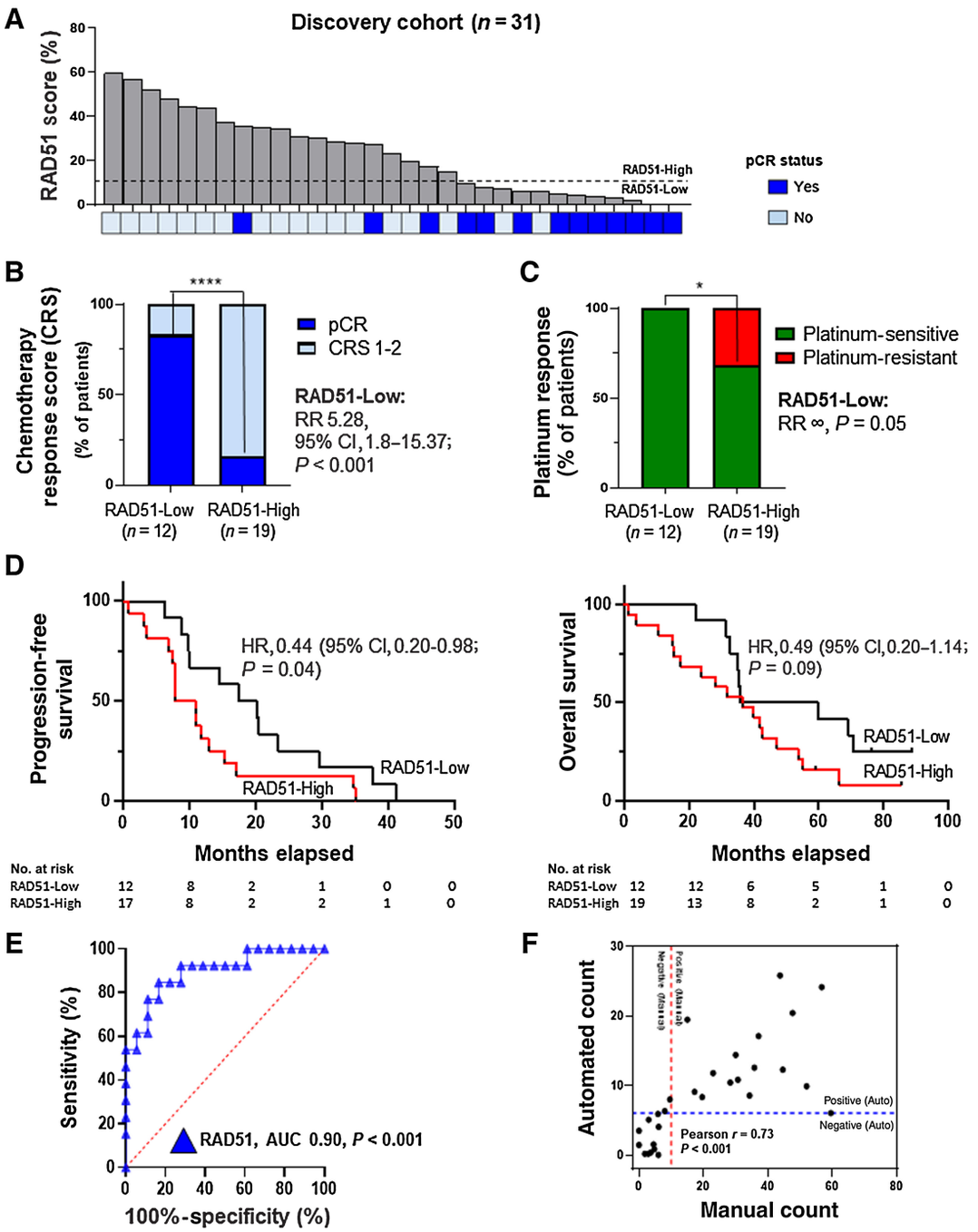

Figure 3.

RAD51 score predicts platinum chemotherapy response and survival in ovarian cancer in a discovery cohort. **A,** RAD51 score and pathologic complete response (pCR) in patients with high-grade serous ovarian cancer before neoadjuvant chemotherapy. Dotted black line indicates manual quantification 10% cutoff value, which delineates RAD51-High and RAD51-Low tumors. All foci were counted in $n > 100$ geminin-positive cells per experiment. Technical replicates were performed for 30% of samples. **B,** Proportion of pretreatment RAD51-Low ($n = 12$) and RAD51-High ($n = 19$) tumors that had a pCR versus chemotherapy response score of 1–2 (RR, 5.28; 95% CI, 1.8–15.37; $P < 0.001$). **C,** Proportion of pretreatment RAD51-Low ($n = 12$) and RAD51-High ($n = 19$) tumors that were platinum-sensitive versus resistant (RR ∞, $P = 0.05$). *, $P < 0.05$ and ****, $P < 0.0001$ by the Student two-tailed t test **D,** Kaplan–Meier curves evaluating progression-free survival (left) and overall survival (right) in patients ($n = 31$) stratified by RAD51 scores. **E,** Receiver operating characteristic curve evaluating the predictive performance of RAD51 score and pathologic complete response. **F,** Correlation between manual quantification and novel automated quantification in patient-derived FFPE tumor samples.

internal control, we calculated γH2AX and RAD51 scores for all benign tissue. γH2AX scores were noted to be <25%, and RAD51 scores were consistently less than 10 (mean 4.5 ± 4.6). γH2AX scores were >25% for 148/149 (99.3%) tumors analyzed. Primary tumor samples were used for analysis when available ($n = 141$). Metastatic tumors ($n = 7$) were used when primary samples were unavailable. A broad range of RAD51 scores was noted (0.8–56.9%; **Fig. 4A**). Thirty-four (22.9%) tumors were RAD51-Low and 114 (77.1%) were RAD51-High (Supplementary Table S5). RAD51-Low tumors were more likely to be platinum-sensitive than RAD51-High tumors (100% vs. 73.1%, $P = 0.005$; RR ∞, $P < 0.001$; **Fig. 4B**). On multivariate analysis, patients with RAD51-Low tumors had significantly longer PFS (20.0 vs. 10.0 months; HR, 0.53; 95% CI, 0.33–0.85; $P = 0.008$; **Fig. 4C**) and OS (123.2 vs. 70.8 months; HR, 0.43; 95% CI, 0.25–0.75; $P = 0.003$; **Fig. 4D**) than patients with RAD51-High tumors when controlling for stage and residual disease at time of cytoreductive surgery. Overall, RAD51 scores in metastatic tumors showed fair correlation with RAD51 scores in primary tumors (Cohen's Kappa coefficient 0.3, $P < 0.001$). On univariate analysis, RAD51-Low score in primary tumors was more strongly associated with survival than RAD51-Low score in metastatic tumors (HR, 0.47; 95% CI, 0.29–0.76; $P = 0.002$ vs. HR, 1.2; 95% CI, 0.77–0.1.88; $P = 0.4$;

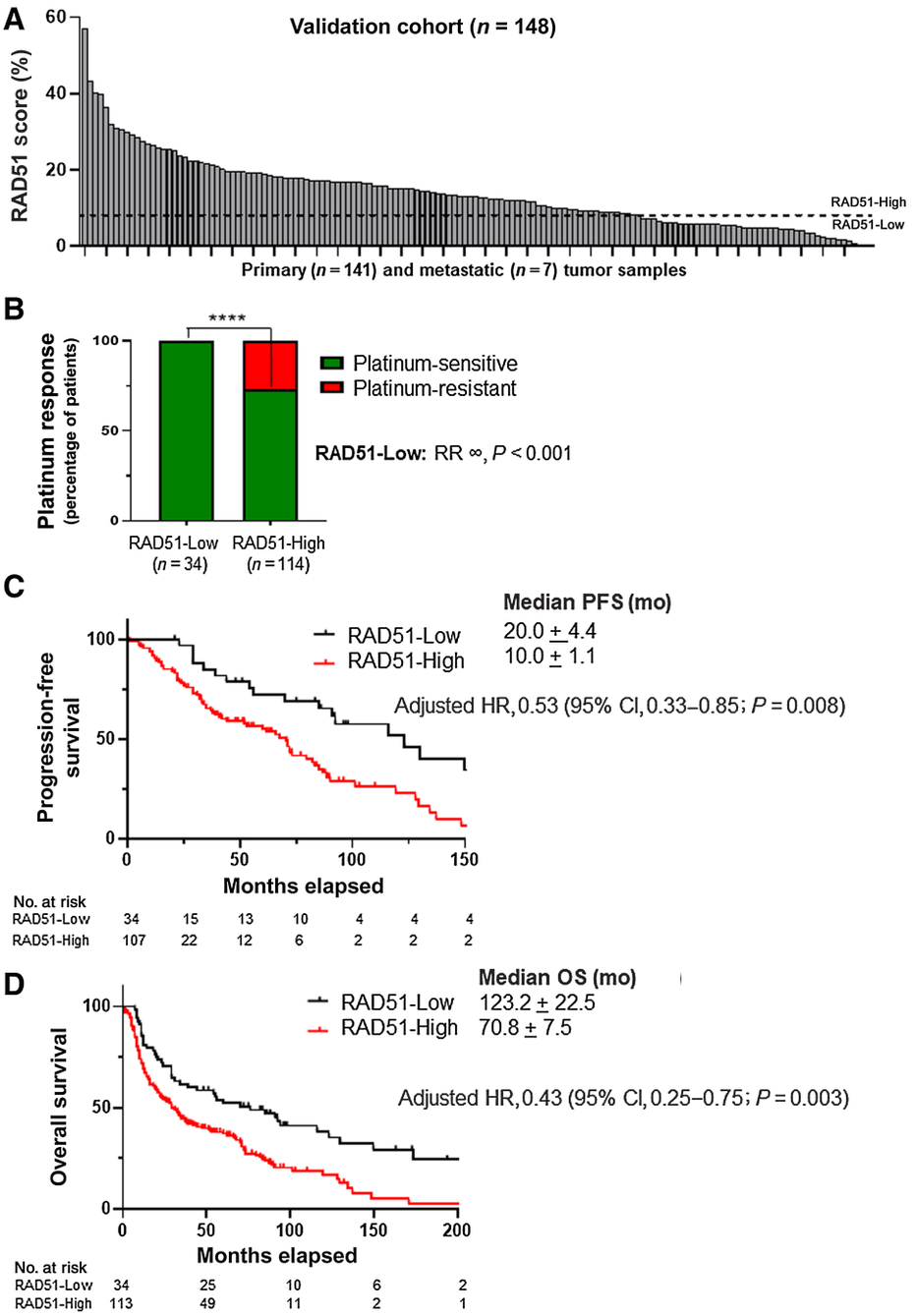

Figure 4.

Automated RAD51 scores predict platinum chemotherapy response and survival in a validation cohort. **A,** RAD51 score in patients with high-grade serous ovarian cancer before ($n = 126$) or after ($n = 22$) 3 cycles of neoadjuvant chemotherapy. Primary tumors were scored when possible ($n = 141$) and metastatic tumors when primary samples were unavailable ($n = 7$). Dotted black line indicates automatic quantification 6% cutoff value, which delineates RAD51-High and RAD51-Low tumors. All foci were counted using automated software. **B,** Proportion of RAD51 RAD51-Low ($n = 34$) and RAD51-High ($n = 114$) tumors that were platinum-sensitive versus resistant (RR ∞, $P < 0.001$). ****, $P < 0.0001$ by Student two-tailed t test. **C,** Kaplan–Meier curves evaluating progression-free survival in patients ($n = 141$) stratified by RAD51 scores. **D,** Kaplan–Meier curves evaluating overall survival in patients ($n = 147$) stratified by RAD51 scores.

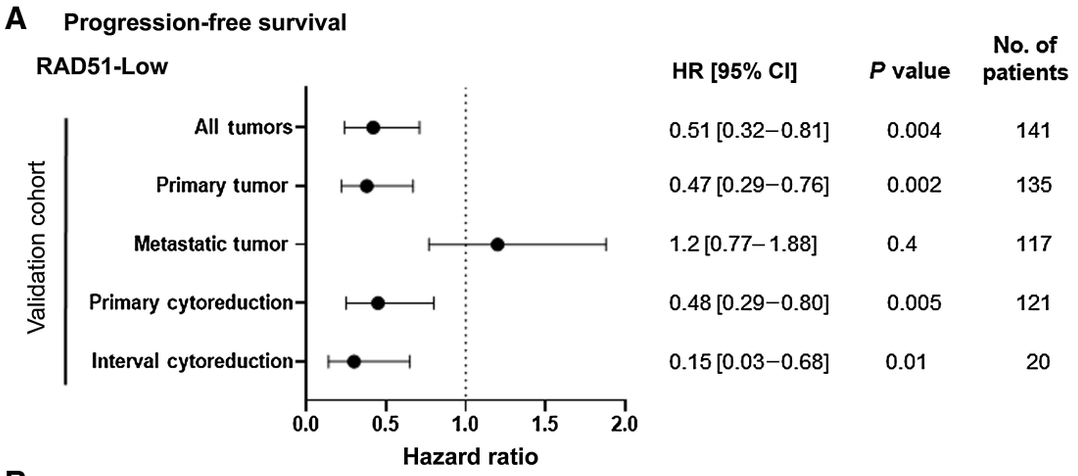

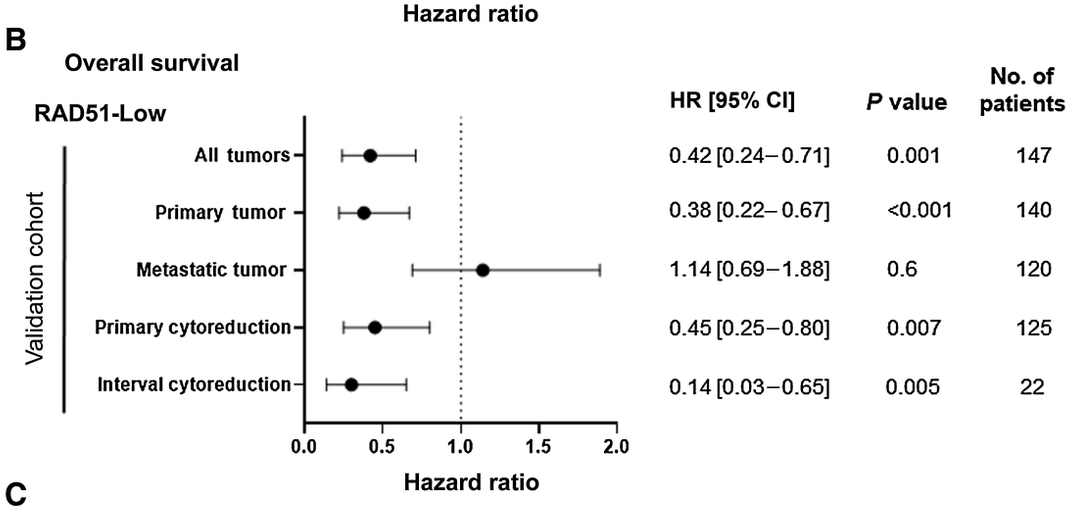

C

Biomarker of Platinum sensitivity	Discovery cohort RAD51-Low (*n* = 31)	Validation cohort RAD51-Low (*n* = 148)
Specificity	100%	100%
Sensitivity	48.0%	30.1%
PPV	100%	100%
NPV	31.6%	26.9%

Figure 5.

RAD51-Low tumors predict platinum sensitivity. **A,** Forest plot with univariate hazard ratios and 95% confidence intervals (CIs) evaluating association between progression-free survival and RAD51-Low scores in different tumor samples. Analysis performed on the validation cohort. **B,** Forest plot with univariate hazard ratios and 95% CIs evaluating association between overall survival and RAD51-Low scores in different tumor samples. Analysis performed on the validation cohort. **C,** Sensitivity, specificity, PPV, and NPV for RAD51-Low tumors in predicting platinum sensitivity in both the discovery ($n = 31$) and validation cohorts ($n = 148$).

Fig. 5A and **B**). RAD51-Low scores in tumor samples obtained from both primary and interval cytoreductive surgery were associated with survival (**Fig. 5A** and **B**).

Overall, a RAD51-Low score predicted platinum sensitivity with 30% to 48% sensitivity, 100% specificity, and 100% positive predictive value in both discovery and validation cohorts (**Fig. 5C**).

Discussion

Current biomarkers of platinum chemotherapy response in HGSOC have limitations. We provide several lines of novel evidence that RAD51 foci are clinically valid and can accurately predict response to platinum chemotherapy in ovarian cancer samples with great precision. First, we show that a RAD51 foci assay can accurately

predict platinum chemotherapy response in established and patient-derived ovarian cancer cell lines and patient-derived ovarian cancer organoids. In line with other studies evaluating RAD51 foci in patient-derived xenografts and cells, we found that in total approximately 25% of HGSOC tumors are RAD51-Low (9, 31). Second, we show that our methods can reproducibly provide a RAD51 score in HGSOC FFPE tissue. Third, we establish that RAD51 foci are predictive of platinum chemotherapy response using novel automated quantification in a collection of 31 FFPE pretreatment ovarian tumor samples. Finally, we validate these findings in a cohort of 148 tumors samples. We demonstrate that RAD51 foci can predict platinum sensitivity with 100% specificity and 100% positive predictive value.

We interpret our findings in HGSOC cells, organoids, and patient FFPE samples as follows: RAD51 foci formation reflects proficiency in many upstream HR events and thus is a well-established readout for HR proficiency (39, 40). Because platinum chemotherapy causes dsDNA breaks in the S-phase due to interstrand lesions as well as intrastrand lesions undergoing nucleotide excision repair, cells that cannot form RAD51 foci cannot use HR to repair DNA and thus die in response to chemotherapy (41, 42). As a result, the RAD51-Low cells and organoids are platinum-responsive, and patients with RAD51-Low tumors are more likely than those with RAD51-High tumors to show a good response to platinum chemotherapy. In conclusion, although platinum sensitivity is multifactorial and the result of diverse cellular processes, including drug uptake, DNA damage signaling, nucleotide excision repair, cell-cycle checkpoints, and cell death pathways (43), our results support RAD51 as a biomarker predictive of response to platinum chemotherapy in ovarian cancer.

RAD51 foci offer an extremely valuable tool for clinical decision making. As almost every patient with ovarian cancer is treated with platinum chemotherapy, it is important to identify patients who will certainly benefit from standard-of-care chemotherapy to avoid unnecessary toxicity of ineffective drugs and to maximize the benefit received from specific therapies. Our results show that the probability of a patient with a RAD51-Low tumor demonstrating platinum sensitivity is 100%. These results are unprecedented for a biomarker predictive of platinum chemotherapy response in ovarian cancer and offer great promise for the precise treatment of this disease.

Our findings are consistent with other reports that *BRCA* mutation status alone does not unequivocally determine platinum chemotherapy response. Similar to Gorodnova and colleagues (44), we found that patients with *BRCA* mutations had longer survival and about 40% of these patients achieved a pCR (44–46). Within the discovery cohort, 44% ($n = 4$) of tumors with *BRCA* mutations were scored as RAD51-High, and these patients all had poor responses to platinum chemotherapy and decreased survival. Given limited data regarding *BRCA* mutation pathogenicity in our validation cohort, it is difficult to draw further conclusions regarding the use of this assay in a cohort of patients with *BRCA* mutations. Nonetheless, data from the discovery cohort confirm findings from prospective clinical trials such as SOLO1 and PRIMA that there is a subset of *BRCA*-mutated patients who do not respond as expected to DNA damaging therapy (45, 46). Possible explanations for differences in chemotherapy response in *BRCA*-mutated tumors include restoration of BRCA function by, for example, hypomorphic protein expression, stabilization of the BRCA1 C-terminal domain, alternative splicing or alternative translation initiation of *BRCA* genes, reversion mutations, or by dysregulation of DSB end resection, including loss of 53BP1 (47–51). Exploratory analysis of our samples suggest increased BRCA mRNA and increased BRCA foci in at least a portion of our RAD51-High *BRCA* mutated samples. Further work is necessary to understand the mechanisms behind differential responses in these cells, but our results support further study of the incorporation of RAD51 foci within the current standard-of-care genomic biomarkers.

In this work, we overcame several potential limitations of a RAD51-based assay for assessing ovarian cancer samples. FFPE samples are the most accessible source for patients' tumors, as formalin fixation is a standard procedure performed routinely in pathology laboratories. However, formalin fixation affects tissue antigens through the formation of methylene bridges that modify protein conformation and epitopes, resulting in poor antibody reactivity. To ensure the immunoreactivity of the fixed antigens (γH2AX, Geminin, RAD51) in our assays, we first carefully validated antigen retrieval steps (antigen retrieval buffer, temperature, and time) and specificity of antibodies in FFPE cell lines. Second, this assay is technically challenging. However, we demonstrate reproducible, optimized methods adapted from investigations in other cancer types and patient-derived xenograft models (13, 52). We validated our assay in prospectively obtained HGSOC samples (53). We observed 2 factors that affected RAD51 staining quality. Samples that were 3 to 4 μm thick provided the best image quality. In addition, biopsies that were of the primary tumor and immediately placed in fixative had higher quality results than samples from large tissue collections such as a cytoreduction surgery obtained from metastatic sites. A third potential limitation of the RAD51 foci assay was that previous studies suggested significant tumor heterogeneity in RAD51 scores (31). Although we observed this in our validation cohort, this was not noted in the discovery cohort. In our discovery cohort, we evaluated 4 quadrants of an entire tumor slide as opposed to small tumor biopsies on a microarray in the validation cohort. Therefore, we hypothesize that tumor heterogeneity can be overcome by evaluating larger tumor samples. Nonetheless, on the basis of our findings, the primary tumor should be evaluated for RAD51 score when possible. Finally, manual counting of RAD51 foci can be subjective and time consuming. Thus, we developed an automated image processing method to quantify RAD51 foci and observed a strong correlation with the manual quantification. This automated scoring system both removes bias from the assay and once validated, will allow this assay to be widely implemented in histopathology laboratories.

We note 3 important limitations of our study. First, a proportion of platinum-sensitive tumors were RAD51-High. Therefore, further investigation is necessary to more accurately stratify RAD51-High tumors. Second, tumor samples were only obtained at cytoreductive surgery, and so we are unable to make conclusions regarding the use of this biomarker throughout a patient's treatment course to determine the utility of a repeat challenge with platinum chemotherapy. In addition, our study focused on the correlation between RAD51 foci and platinum response. However, given the importance of HR status in PARPi response, future work should assess the ability of the RAD51 foci assay to predict PARPi response.

In conclusion, we demonstrate that RAD51 is a robust and reliable biomarker predictive of response to platinum chemotherapy. Further studies are needed to prospectively evaluate this biomarker for translation into clinical care.

Authors' Disclosures

A. Llop-Guevara reports grants from Asociación Española Contra el Cáncer (AECC, INVES20095LLOP) during the conduct of the study and reports a patent for WO2019122411A1 pending. A. Herencia-Ropero reports grants from Generalitat de Catalunya (PERIS) during the conduct of the study. S.P. Harrington reports grants from Ovarian Cancer Research Alliance and grants from National Institutes of Health, TL1 during the conduct of the study. L.M. Kuroki reports grants from NIH—R03,

Washington University Implementation Science Center for Cancer Control—P20 pilot grant, Doris Duke Foundation, other support from GOG-Foundation, personal fees from NCI PDQ (editorial board), and nonfinancial support and other support from ASCCP outside the submitted work. P.H. Thaker reports personal fees from Astra Zeneca, GlaxoSmithKline, Clovis Oncology, Merck, Novocure, Immunon, Eisai, Verastem, R Pharm, Aadi Bioscience, and Iovance outside the submitted work. M.A. Powell reports personal fees from Merck, AstraZeneca, SeaGen, GSK, Clovis Oncology, Immunogen, Mersana, and Eisai outside the submitted work. V. Serra reports grants from AstraZeneca and personal fees from GSK outside the submitted work and reports a patent for WO2019122411A1 pending. D. Khabele reports grants from NCI/NIH during the conduct of the study. M.M. Mullen reports grants from The Gynecologic Oncology Group Foundation, Washington University School of Medicine Division of Physician Scientists Dean's Scholar Program, grant 2021265 from the Doris Duke Charitable Foundation through the COVID-19 Fund to Retain Clinical Scientists collaborative grant program, and Reproductive Scientist Development Program during the conduct of the study. No disclosures were reported by the other authors.

Authors' Contributions

A.J. Compadre: Conceptualization, data curation, software, formal analysis, validation, investigation, visualization, methodology, writing–original draft, writing–review and editing. **L.N. van Biljon:** Conceptualization, data curation, software, formal analysis, validation, investigation, visualization, methodology, writing–original draft, writing–review and editing. **M.C. Valentine:** Data curation, software, formal analysis, investigation, writing–original draft, writing–review and editing. **A. Llop-Guevara:** Conceptualization, methodology, writing–review and editing. **E. Graham:** Data curation, software, validation, investigation, visualization, methodology, writing–review and editing. **B. Fashemi:** Methodology, writing–original draft, writing–review and editing. **A. Herencia-Ropero:** Conceptualization, investigation, methodology, writing–review and editing. **E.N. Kotnik:** Data curation, methodology, writing–review and editing. **I. Cooper:** Validation, methodology, writing–review and editing. **S.P. Harrington:** Resources. **L.M. Kuroki:** Resources, data curation, methodology, writing–review and editing. **C.K. McCourt:** Resources, data curation, methodology, writing–review and editing. **A.R. Hagemann:** Resources, data curation, methodology, writing–review and editing. **P.H. Thaker:** Resources, data curation, methodology, writing–review and editing. **D.G. Mutch:** Resources, data curation, funding acquisition, methodology, project administration, writing–review and editing. **M.A. Powell:** Conceptualization, resources, funding acquisition, methodology. **L. Sun:** Validation, methodology, writing–review and editing. **N. Mosammaparast:** Conceptualization, resources, methodology, writing–review and editing. **V. Serra:** Conceptualization, supervision. **P. Zhao:** Software, formal analysis, writing–review and editing. **E. Lomonosova:** Conceptualization, resources, data curation, software, formal analysis, funding acquisition, validation, investigation, methodology, writing–review and editing. **D. Khabele:** Conceptualization, resources, methodology, writing–review and editing. **M.M. Mullen:** Conceptualization, resources, data curation, software, formal analysis, supervision, funding acquisition, validation, investigation, visualization, methodology, project administration.

Acknowledgments

We thank Katherine Fuh for her extensive ongoing mentorship and supplying one of the tissue microarrays used for this study. We also thank Deborah Frank for her article editing, Anthony Bartley for generating illustrations and editing figures, and Priyanka Verma and Abby Green for input regarding experimental design and article editing. Finally, we would like to acknowledge the Washington University Gynecologic Oncology Biorepository for their contributions. This work was supported by the following entities: M. Mullen reports funding from the Reproductive Scientist Development Program (RSDP) supported by the Gynecologic Oncology Group Foundation, Washington University School of Medicine Division of Physician Scientists Dean's Scholar Program, and grant 2021265 from the Doris Duke Charitable Foundation through the COVID-19 Fund to Retain Clinical Scientists collaborative grant program. D. Khabele reports funding from RO1CA243511, University of Kansas Cancer Center P30 CA168524. D.G. Mutch reports funding from Washington University School of Medicine grant 5U1-CA180860–04.

The publication costs of this article were defrayed in part by the payment of publication fees. Therefore, and solely to indicate this fact, this article is hereby marked "advertisement" in accordance with 18 USC section 1734.

Note

Supplementary data for this article are available at Clinical Cancer Research Online (http://clincancerres.aacrjournals.org/).

Received October 31, 2022; revised January 31, 2023; accepted April 20, 2023; published first April 25, 2023.

References

1. Lheureux S, Gourley C, Vergote I, Oza AM. Epithelial ovarian cancer. Lancet 2019;393:1240–53.
2. Tew WP, Lacchetti C, Ellis A, Maxian K, Banerjee S, Bookman M, et al. PARP inhibitors in the management of ovarian cancer: ASCO guideline. J Clin Oncol 2020;38:3468–93.
3. Pennington KP, Walsh T, Harrell MI, Lee MK, Pennil CC, Rendi MH, et al. Germline and somatic mutations in homologous recombination genes predict platinum response and survival in ovarian, fallopian tube, and peritoneal carcinomas. Clin Cancer Res 2014;20:764–75.
4. Swisher EM, Lin KK, Oza AM, Scott CL, Giordano H, Sun J, et al. Rucaparib in relapsed, platinum-sensitive high-grade ovarian carcinoma (ARIEL2 part 1): an international, multicentre, open-label, phase 2 trial. Lancet Oncol 2017;18:75–87.
5. Mirza MR, Monk BJ, Herrstedt J, Oza AM, Mahner S, Redondo A, et al. Niraparib maintenance therapy in platinum-sensitive, recurrent ovarian cancer. N Engl J Med 2016;375:2154–64.
6. Ceccaldi R, Rondinelli B, D'Andrea AD. Repair pathway choices and consequences at the double-strand break. Trends Cell Biol 2016;26:52–64.
7. Wilson AJ, Stubbs M, Liu P, Ruggeri B, Khabele D. The BET inhibitor INCB054329 reduces homologous recombination efficiency and augments PARP inhibitor activity in ovarian cancer. Gynecol Oncol 2018;149:575–84.
8. Ito K, Murayama Y, Kurokawa Y, Kanamaru S, Kokabu Y, Maki T, et al. Real-time tracking reveals catalytic roles for the two DNA binding sites of Rad51. Nat Commun 2020;11:2950.
9. Pellegrino B, Herencia-Ropero A, Llop-Guevara A, Pedretti F, Moles-Fernández A, Viaplana C, et al. Preclinical *in vivo* validation of the RAD51 test for identification of homologous recombination-deficient tumors and patient stratification. Cancer Res 2022;82:1646–57.
10. Mukhopadhyay A, Elattar A, Cerbinskaite A, Wilkinson SJ, Drew Y, Kyle S, et al. Development of a functional assay for homologous recombination status in primary cultures of epithelial ovarian tumor and correlation with sensitivity to poly(ADP-ribose) polymerase inhibitors. Clin Cancer Res 2010;16:2344–51.
11. Shah MM, Dobbin ZC, Nowsheen S, Wielgos M, Katre AA, Alvarez RD, et al. An *ex vivo* assay of XRT-induced Rad51 foci formation predicts response to PARP-inhibition in ovarian cancer. Gynecol Oncol 2014;134:331–7.
12. Graeser M, McCarthy A, Lord CJ, Savage K, Hills M, Salter J, et al. A marker of homologous recombination predicts pathologic complete response to neoadjuvant chemotherapy in primary breast cancer. Clin Cancer Res 2010;16:6159–68.
13. Llop-Guevara A, Loibl S, Villacampa G, Vladimirova V, Schneeweiss A, Karn T, et al. Association of RAD51 with homologous recombination deficiency (HRD) and clinical outcomes in untreated triple-negative breast cancer (TNBC): analysis of the GeparSixto randomized clinical trial. Ann Oncol 2021;32:1590–6.
14. Böhm S, Faruqi A, Said I, Lockley M, Brockbank E, Jeyarajah A, et al. Chemotherapy response score: development and validation of a system to quantify histopathologic response to neoadjuvant chemotherapy in tubo-ovarian high-grade serous carcinoma. J Clin Oncol 2015;33:2457–63.
15. Petrillo M, Zannoni GF, Tortorella L, Pedone Anchora L, Salutari V, Ercoli A, et al. Prognostic role and predictors of complete pathologic response to neoadjuvant chemotherapy in primary unresectable ovarian cancer. Am J Obstet Gynecol 2014;211:632.e1–8.
16. Le T, Shahriari P, Hopkins L, Faught W, Fung Kee Fung M. Prognostic significance of tumor necrosis in ovarian cancer patients treated with neoadjuvant chemotherapy and interval surgical debulking. Int J Gynecol Cancer 2006;16:986–90.

17. Le T, Williams K, Senterman M, Hopkins L, Faught W, Fung-Kee-Fung M. Omental chemotherapy effects as a prognostic factor in ovarian cancer patients treated with neoadjuvant chemotherapy and delayed primary surgical debulking. Ann Surg Oncol 2007;14:2649–53.
18. Muraji M, Sudo T, Iwasaki S, Ueno S, Wakahashi S, Yamaguchi S, et al. Histopathology predicts clinical outcome in advanced epithelial ovarian cancer patients treated with neoadjuvant chemotherapy and debulking surgery. Gynecol Oncol 2013;131:531–4.
19. Sassen S, Schmalfeldt B, Avril N, Kuhn W, Busch R, Hofler H, et al. Histopathologic assessment of tumor regression after neoadjuvant chemotherapy in advanced-stage ovarian cancer. Hum Pathol 2007;38:926–34.
20. de Luca XM, Newell F, Kazakoff SH, Hartel G, McCart Reed AE, Holmes O, et al. Using whole-genome sequencing data to derive the homologous recombination deficiency scores. NPJ Breast Cancer 2020;6:33.
21. Denkert C, Romey M, Swedlund B, Hattesohl A, Teply-Szymanski J, Kommoss S, et al. Homologous recombination deficiency as an ovarian cancer biomarker in a real-world cohort: validation of decentralized genomic profiling. J Mol Diagn 2022;24:1254–63.
22. Telli ML, Hellyer J, Audeh W, Jensen KC, Bose S, Timms KM, et al. Homologous recombination deficiency (HRD) status predicts response to standard neoadjuvant chemotherapy in patients with triple-negative or BRCA1/2 mutation-associated breast cancer. Breast Cancer Res Treat 2018;168:625–30.
23. Telli ML, Timms KM, Reid J, Hennessy B, Mills GB, Jensen KC, et al. Homologous Recombination Deficiency (HRD) score predicts response to platinum-containing neoadjuvant chemotherapy in patients with triple-negative breast cancer. Clin Cancer Res 2016;22:3764–73.
24. Monk BJ, Coleman RL, Fujiwara K, Wilson MK, Oza AM, Oaknin A, et al. ATHENA (GOG-3020/ENGOT-ov45): a randomized, phase III trial to evaluate rucaparib as monotherapy (ATHENA-MONO) and rucaparib in combination with nivolumab (ATHENA-COMBO) as maintenance treatment following frontline platinum-based chemotherapy in ovarian cancer. Int J Gynecol Cancer 2021;31:1589–94.
25. Coleman RL, Oza AM, Lorusso D, Aghajanian C, Oaknin A, Dean A, et al. Rucaparib maintenance treatment for recurrent ovarian carcinoma after response to platinum therapy (ARIEL3): a randomised, double-blind, placebo-controlled, phase 3 trial. Lancet 2017;390:1949–61.
26. Bray NL, Pimentel H, Melsted P, Pachter L. Near-optimal probabilistic RNA-seq quantification. Nat Biotechnol 2016;34:525–7.
27. Jakl L, Lobachevsky P, Vokálová L, Durdík M, Marková E, Belyaev I. Validation of JCountPro software for efficient assessment of ionizing radiation-induced foci in human lymphocytes. Int J Radiat Biol 2016;92:766–73.
28. Ivashkevich AN, Martin OA, Smith AJ, Redon CE, Bonner WM, Martin RF, et al. γH2AX foci as a measure of DNA damage: a computational approach to automatic analysis. Mutat Res 2011;711:49–60.
29. Hill SJ, Decker B, Roberts EA, Horowitz NS, Muto MG, Worley MJ Jr, et al. Prediction of DNA repair inhibitor response in short-term patient-derived ovarian cancer organoids. Cancer Discov 2018;8:1404–21.
30. Davis A, Tinker AV, Friedlander M. Platinum-resistant ovarian cancer: what is it, who to treat and how to measure benefit? Gynecol Oncol 2014;133:624–31.
31. Tumiati M, Hietanen S, Hynninen J, Pietilä E, Färkkilä A, Kaipio K, et al. A functional homologous recombination assay predicts primary chemotherapy response and long-term survival in ovarian cancer patients. Clin Cancer Res 2018;24:4482–93.
32. Hoppe MM, Jaynes P, Wardyn JD, Upadhyayula SS, Tan TZ, Lie S, et al. Quantitative imaging of RAD51 expression as a marker of platinum resistance in ovarian cancer. EMBO Mol Med 2021;13:e13366.
33. Woodward M. Formulae for sample size, power and minimum detectable relative risk in medical studies. J Royal Stat Soc 1992;41:185–96.
34. Meijer TG, Verkaik NS, Sieuwerts AM, van Riet J, Naipal KAT, van Deurzen CHM, et al. Functional ex vivo assay reveals homologous recombination deficiency in breast cancer beyond BRCA gene defects. Clin Cancer Res 2018;24:6277–87.
35. Barretina J, Caponigro G, Stransky N, Venkatesan K, Margolin AA, Kim S, et al. The cancer cell line encyclopedia enables predictive modelling of anticancer drug sensitivity. Nature 2012;483:603–7.
36. Yang W, Soares J, Greninger P, Edelman EJ, Lightfoot H, Forbes S, et al. Genomics of Drug Sensitivity in Cancer (GDSC): a resource for therapeutic biomarker discovery in cancer cells. Nucleic Acids Res 2012;41:D955–D61.
37. Mullen MM, Lomonosova E, Toboni MD, Oplt A, Cybulla E, Blachut B, et al. GAS6/AXL inhibition enhances ovarian cancer sensitivity to chemotherapy and PARP inhibition through increased DNA damage and enhanced replication stress. Mol Cancer Res 2022;20:265–79.
38. Mukaka MM. Statistics corner: a guide to appropriate use of correlation coefficient in medical research. Malawi Med J 2012;24:69–71.
39. Yazinski SA, Comaills V, Buisson R, Genois MM, Nguyen HD, Ho CK, et al. ATR inhibition disrupts rewired homologous recombination and fork protection pathways in PARP inhibitor-resistant BRCA-deficient cancer cells. Genes Dev 2017;31:318–32.
40. Orthwein A, Noordermeer SM, Wilson MD, Landry S, Enchev RI, Sherker A, et al. A mechanism for the suppression of homologous recombination in G1 cells. Nature 2015;528:422–6.
41. Reardon JT, Vaisman A, Chaney SG, Sancar A. Efficient nucleotide excision repair of cisplatin, oxaliplatin, and Bis-aceto-ammine-dichloro-cyclohexyl-amine-platinum(IV) (JM216) platinum intrastrand DNA diadducts. Cancer Res 1999;59:3968–71.
42. Rottenberg S, Disler C, Perego P. The rediscovery of platinum-based cancer therapy. Nat Rev Cancer 2021;21:37–50.
43. Wang D, Lippard SJ. Cellular processing of platinum anticancer drugs. Nat Rev Drug Discovery 2005;4:307–20.
44. Gorodnova TV, Kotiv KB, Ivantsov AO, Mikheyeva ON, Mikhailiuk GI, Lisyanskaya AS, et al. Int J Gynecol Cancer 2018;28:1498–506.
45. Moore K, Colombo N, Scambia G, Kim BG, Oaknin A, Friedlander M, et al. Maintenance olaparib in patients with newly diagnosed advanced ovarian cancer. N Engl J Med 2018;379:2495–505.
46. González-Martín A, Pothuri B, Vergote I, DePont Christensen R, Graybill W, Mirza MR, et al. Niraparib in patients with newly diagnosed advanced ovarian cancer. N Engl J Med 2019;381:2391–402.
47. Noordermeer SM, van Attikum H. PARP inhibitor resistance: a tug-of-war in BRCA-mutated cells. Trends Cell Biol 2019;29:820–34.
48. Fuh K, Mullen M, Blachut B, Stover E, Konstantinopoulos P, Liu J, et al. Homologous recombination deficiency real-time clinical assays, ready or not? Gynecol Oncol 2020;159:877–86.
49. Norquist B, Wurz KA, Pennil CC, Garcia R, Gross J, Sakai W, et al. Secondary somatic mutations restoring BRCA1/2 predict chemotherapy resistance in hereditary ovarian carcinomas. J Clin Oncol 2011;29:3008–15.
50. Hurley RM, Wahner Hendrickson AE, Visscher DW, Ansell P, Harrell MI, Wagner JM, et al. 53BP1 as a potential predictor of response in PARP inhibitor-treated homologous recombination-deficient ovarian cancer. Gynecol Oncol 2019;153:127–34.
51. Sakai W, Swisher EM, Karlan BY, Agarwal MK, Higgins J, Friedman C, et al. Secondary mutations as a mechanism of cisplatin resistance in BRCA2-mutated cancers. Nature 2008;451:1116–20.
52. Castroviejo-Bermejo M, Cruz C, Llop-Guevara A, Gutiérrez-Enríquez S, Ducy M, Ibrahim YH, et al. A RAD51 assay feasible in routine tumor samples calls PARP inhibitor response beyond BRCA mutation. EMBO Mol Med 2018;10:e9172.
53. Altman DG, McShane LM, Sauerbrei W, Taube SE. Reporting recommendations for tumor marker prognostic studies (REMARK): explanation and elaboration. BMC Medicine 2012;10:51.